

Energy: Photovoltaics, Energy Harvesting, Energy Storage

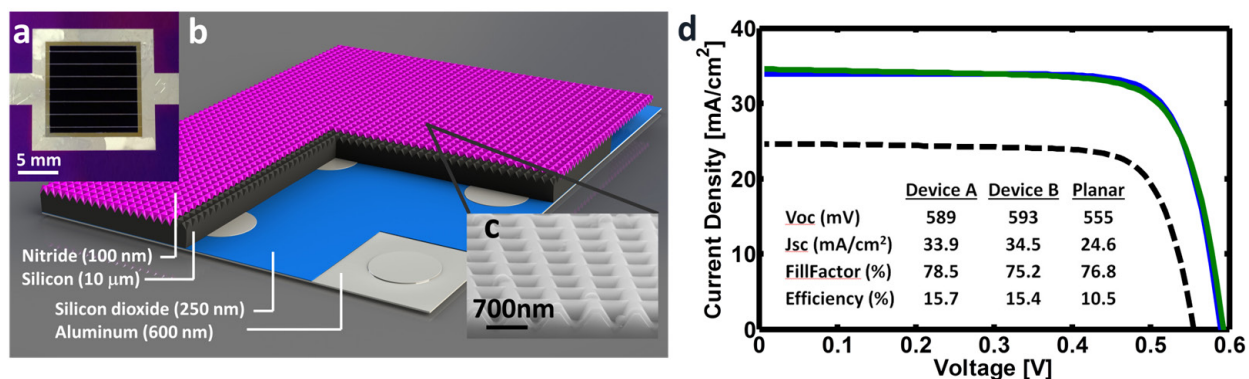
15.7% Efficient 10- μ m-Thick Crystalline Silicon Solar Cells	61
Surface Passivation of Silicon using Organic Molecules.....	62
Utilization of BaSnO ₃ and Related Materials Systems for Transparent Conducting Electrodes.....	63
Ink-Jet Printing of Organic-Inorganic Halide Perovskites for Solar Photovoltaics.....	64
Open-Circuit Voltage Deficit, Radiative Sub-Bandgap States, and Prospects in Quantum Dot Solar Cells.....	65
Control of the Fermi Level of Lead Sulfide Quantum Dots through Ligand Steric Interactions	66
<i>In Situ</i> Vapor-Deposited Parylene Substrates for Ultra-Thin, Lightweight Organic Solar Cells.....	67
Solid State Triplet-Triplet Annihilation Upconversion	68
Thin Film Evaporation from Nanopores and its Applications to Solar Thermal Devices.....	69
MEMS Energy Harvesting from Low-Frequency and Low-G Vibrations.....	70
Fabrication of Ruthenium Oxide-Coated Si Nanowire-Based Supercapacitors	71
Materials and Structures for Lithium-Air Batteries	72
Mechanical Stresses in Germanium Thin Film Microbattery Electrodes during Cycling	73
Oxygen Exchange Kinetics in Pr ₂ CuO ₄ Thin Film Cathodes: The Role of Doping and Orientation.....	74
Development of Reversible Solid Oxide Cells: A Search for New Electrode Materials.....	75
Investigation of Fuel Cell Cathode Performance in Solid Oxide Fuel Cells: Application of Model Thin Film Structures.....	76
Fundamental Studies of Oxygen Exchange and Associated Expansion in Solid Oxide Fuel Cell Cathodes	77

15.7% Efficient 10- μm -Thick Crystalline Silicon Solar Cells

M. S. Branham, W. C. Hsu, S. Yerci, S. V. Boriskina, G. Chen
Sponsorship : SunShot Initiative, Department of Energy

As the cost of crystalline silicon solar cell modules has steadily declined in recent years, the proportion of the module cost attributable to silicon has remained stubbornly high, accounting for 30% - 40% of the total. One promising approach to cutting the silicon cost component of solar modules is utilizing new manufacturing strategies such as epitaxial silicon growth on porous silicon or direct wafering to reduce the volume of silicon used in a photovoltaic cell. This strategy in particular has sparked a flurry of research addressing an impediment to the realization of ultrathin crystalline silicon cells: how to maintain competitively high efficiencies while shrinking the volume of silicon available to absorb incident photons. We overcome this challenge by incorporating a light-trapping nanostructure into an ultrathin silicon film, resulting in a substantial advance in short-circuit current and efficiency over previous efforts. We demonstrated experimentally that an inverted nanopyramid light-trapping scheme

for a 10- μm -thick c-Si thin-film can achieve 15.7% energy conversion efficiency and 34.5 mA/cm² short-circuit current using a periodic inverted nano-pyramids structure. We have also demonstrated experimentally that even random texturing can lead to good light-trapping characteristics. To reach the high efficiencies necessary for a commercial product, we also constructed a multi-physics optimization tool incorporating both optical absorption and electronic carrier collection to understand in detail the loss mechanisms of the devices, including incomplete photonic absorption, contact recombination, surface recombination, and Schottky-Read-Hall and Auger recombination. Our model predicts that a 10- μm -thick thin-film c-Si solar cell can have an efficiency approaching 20% as the electronic properties are improved.



▲ Figure 1: 15.7% Efficient 10- μm -thick crystalline silicon solar cells using periodic nanostructures. (a) The top view of the solar device with an active area of 1cm x 1cm. (b) The schematic of structures. (c) Scanning electron microscope image of 700-nm-pitch inverted nano-pyramids light-trapping structure. (d) Performance (Current-voltage curves) of the solar devices and a planar (untextured) reference device.

FURTHER READING

- S. E. Han and G. Chen. *Nano Letters*. 10, 4692-4696, 2010.
- A. Mavrokefalos, S. E. Han, S. Yerci, M. S. Branham, and G. Chen. *Nano Letters*. 12, 2792-2796, 2012.
- M. S. Branham, W.-C. Hsu, S. Yerci, J. Loomis, S. V. Boriskina, B. R. Hoard, S. E. Han, and G. Chen. *Adv. Mater.* 27, 2182-2188, 2015.

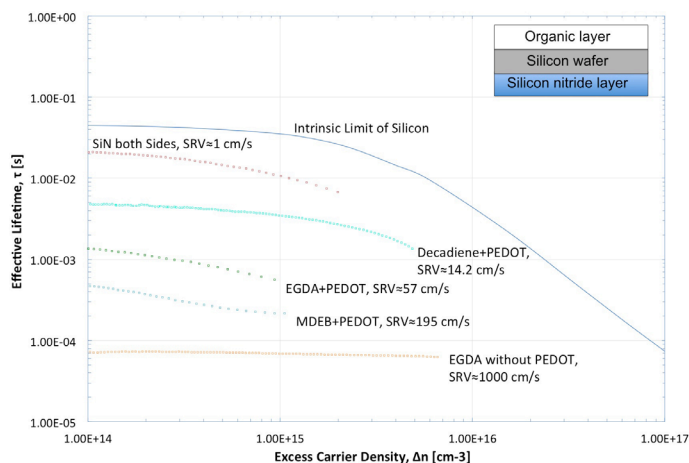
Surface Passivation of Silicon using Organic Molecules

M. L. Castillo, B. Reeja-Jayan, K. K. Gleason, T. Buonassisi
Sponsorship: EniPower

Many advanced silicon device architectures including photovoltaics and integrated circuits require excellent surface passivation. To combine the functionality of polymers with the robustness of silicon technology, we are exploring the direct passivation of silicon with organic molecules. Organic molecules offer a wide range of tunability in size and electronic dipoles and open up new materials for passivation beyond conventional inorganic dielectrics. We use initiated chemical vapor deposition (iCVD) and oxidative chemical vapor deposition (oCVD) to graft these organic molecules on <100>-oriented p-type silicon wafers (B-doped, 80–120 ohm-cm, 750±25 μm thickness). We have observed surface recombination velocities (SRV) of minority carriers as low as 14.2 cm/s and minority carrier lifetimes as high as 4.8 ms, as shown in Figure 1.

We prepared the silicon wafer samples with a silicon nitride passivation layer on the back and an organic passivation layer on the front. In preparation for the silicon nitride passivation, samples went through a Radio Corporation of America (RCA) clean, which is a standard set of wafer-cleaning steps required immediately before any high-temperature process step, to remove organics,

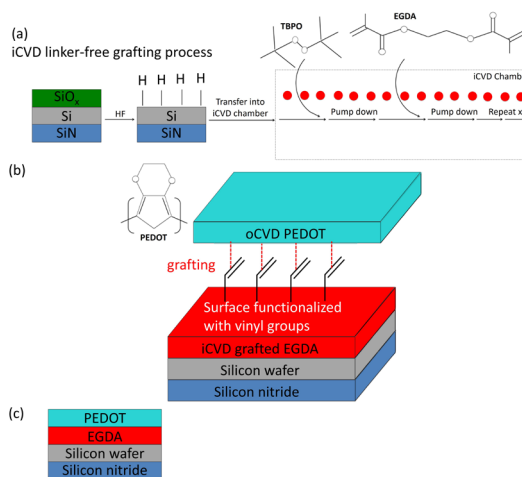
the native oxide, and any remaining extrinsic ions. Then, a 900-Å-thick layer of silicon nitride was deposited at a temperature of 400°C using an Applied Materials Centura 5300 Dielectric Chemical Vapor Deposition (DCVD) tool. After the silicon nitride passivation, we etched the samples in hydrofluoric acid for 2 minutes to remove the native oxide and obtain Si-H on the surface (the densified silicon nitride layer was minimally affected). The samples were then immediately transferred into the (iCVD) chamber (see the ethylene glycol diacetate (EGDA) passivation process in Figure 2 (a)). Finally, poly(3,4-ethylenedioxythiophene) (PEDOT) was deposited via oCVD in another chamber (see Figure 2 (b)). After the organic passivation process, minority-carrier lifetime was measured using a Sinton WCT-120 apparatus. The effective lifetime of various organic passivated layers measured using this tool is shown in Figure 1. Improvement of the quality of the surface passivation of silicon using organic molecules is critical to improving the efficiency of these devices. The combination of PEDOT and decadiene passivation on silicon has resulted in the best surface-passivation quality, as shown in Figure 1.



▲ Figure 1: Effective minority-carrier lifetime(s) of various organic surface passivation layers on silicon and corresponding surface recombination velocity (cm/s) of minority carriers.

FURTHER READING

- R. Yang, T. Buonassisi, and K. K. Gleason, "Organic Vapor Passivation of Silicon at Room Temperature," *Advanced Materials*, vol. 25, pp. 2078-2083, 2013.
- B. Reeja-Jayan, P. Kovacic, R. Yang, H. Sojoudi, A. Ugur, D. H. Kim, C. D. Petruczok, X. Wang, A. Liu, and K. K. Gleason, "A Route Towards Sustainability Through Engineered Polymeric Interfaces," *Advanced Materials Interfaces*, vol. 1, pp. 1400117, 2014.
- B. Reeja-Jayan, P. Moni, and K. K. Gleason, "Synthesis of Insulating and Semiconducting Polymer Films via Initiated Chemical Vapor Deposition," *Nanoscience and Nanotechnology Letters*, vol. 7, pp. 33-38, 2015.



▲ Figure 2: PEDOT on EGDA surface passivation on silicon process via (a) iCVD linker-free grafting process in reactor (Yang, 2013) and (b) oCVD PEDOT layer grafts to vinyl bonds on iCVD grafted EGDA. (c) Example of final device after passivation.

Utilization of BaSnO₃ and Related Materials Systems for Transparent Conducting Electrodes

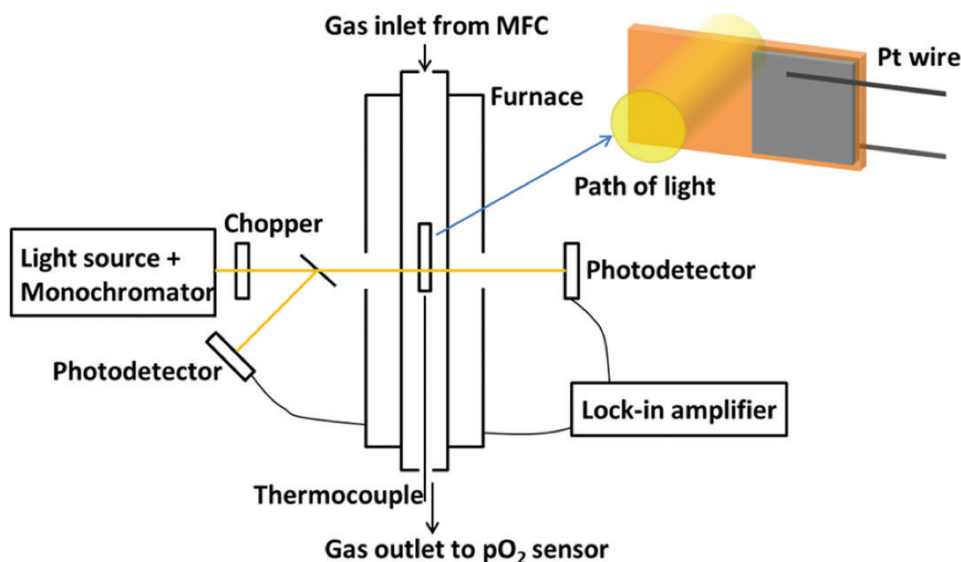
M. Campion, H. L. Tuller

Sponsorship: Department of Energy, Skolkovo Foundation

Efficient transparent electrode materials are vital for applications in smart window, LED display, and solar cell technologies. These materials must possess a wide band gap for minimal optical absorption in the visible spectrum while maintaining a high electrical conductivity. Tin-doped indium oxide (ITO) has been the industry standard for transparent electrodes, but the use of the rare element indium has led to a search for better material alternatives. BaSnO₃ represents a promising alternative due to its high electron mobility and resistance to property degradation under oxidizing conditions, but the mechanisms by which processing conditions and defect chemistry affect the final material properties are not well understood.

This work seeks to better understand the relationships among processing, defect chemistry, and material properties of BaSnO₃, in order to better establish the consistent and controllable use of

BaSnO₃ as a transparent electrode. To accomplish these goals, methods such as *in situ* resistance and impedance monitoring during annealing will be applied. In addition, a variety of novel methods such as the *in situ* monitoring of optical transmission (shown in Figure 1) during annealing and the *in situ* monitoring of resistance during physical vapor deposition will be utilized to investigate BaSnO₃. Direct measurements of the key constants for the thermodynamics and kinetics of oxidation in donor-doped BaSnO₃ will be experimentally determined for the first time. This increase in understanding will provide a predictive model for determining optical properties, carrier concentrations, and electron mobilities in BaSnO₃, which may become increasingly important due to its high electron mobility, high temperature stability, and favorable crystal structure.



▲ Figure 1: Schematic of experimental setup to be used for simultaneous *in situ* measurement of the optical transmission and electrical conductivity of thin film BaSnO₃ samples during annealing under controlled atmosphere and temperature.

FURTHER READING

- D. O. Scanlon, "Defect engineering of BaSnO₃ for high-performance transparent conducting oxide applications," *Phys. Rev. B*, vol. 87, no. 16, p. 161201, Apr. 2013.
- J. J. Kim, S. R. Bishop, N. J. Thompson, D. Chen, and H. L. Tuller, "Investigation of Nonstoichiometry in Oxide Thin Films by Simultaneous *In Situ* Optical Absorption and Chemical Capacitance Measurements: Pr-Doped Ceria, a Case Study," *Chemistry of Materials*, vol. 26, pp. 1374-1379, Jan. 2014.

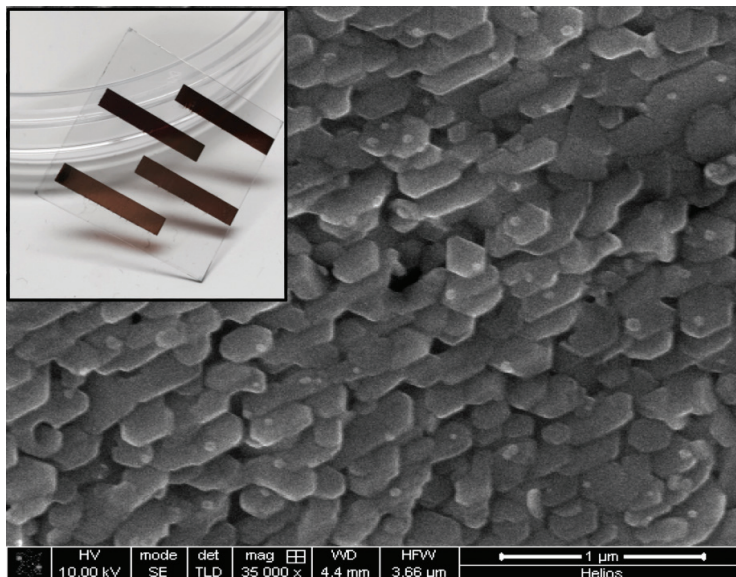
Ink-Jet Printing of Organic-Inorganic Halide Perovskites for Solar Photovoltaics

A. Osherov, S. D. Stranks, M. T. Klug, J. Jean, G. Azzellino, M. C. Sponseller, A. M. Belcher, V. Bulović
Sponsorship: Eni

Remarkable optical and electronic properties, coupled with solution low temperature process-ability and environmental abundance of the precursor materials, have garnered increased attention to the hybrid organic-inorganic, metal halide perovskites as an attractive material alternative for solar photovoltaics.

Low internal losses and efficient carrier transport were demonstrated, and as a result high open-circuit voltages and solar power conversion efficiencies were realized. To achieve large-scale deployment, however, emerging thin-film technologies must achieve high efficiencies using high-throughput manufacturing techniques. Inkjet printing of hybrid organic-inorganic perovskites (e.g., $\text{CH}_3\text{NH}_3\text{PbI}_3$) offers a promising approach for low-cost, scalable manufacturing of future thin-film solar cells.

We are currently investigating the effect of the key printing parameters and precursor solution chemistries on the $\text{CH}_3\text{NH}_3\text{PbI}_3$ film formation, thickness, morphology and homogeneity as well as corresponding photovoltaic performances. Solution engineering allowed control over the evaporation rate and the surface tension gradient, therefore enabling fabrication of dense, continuous films with controlled morphology, as depicted by SEM (Figure 1). Preliminary devices exhibit V_{oc} of 0.86V, J_{sc} of 3.7-6 mA/cm² and η of 3-5%. Further understanding of surface chemistry and wetting behavior are essential for fabrication of efficient photovoltaic devices.



▲ Figure 1: SEM micrograph of ink-jet printed $\text{CH}_3\text{NH}_3\text{PbI}_3$ thin film. Inset: Photograph of the $\text{CH}_3\text{NH}_3\text{PbI}_3$ film on 1" glass substrate, demonstrating mask-less patterning approach.

FURTHER READING

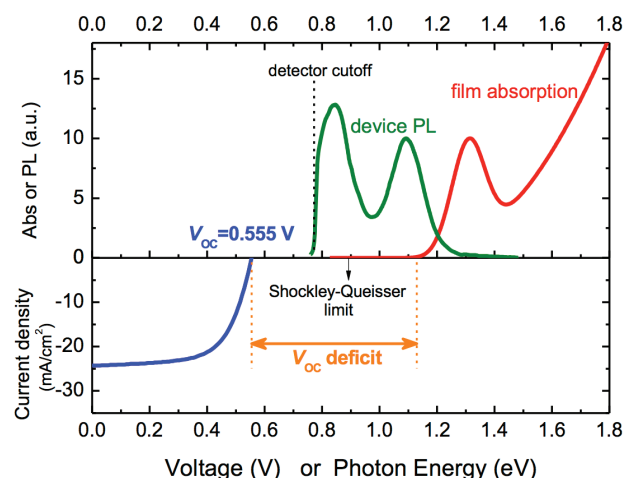
- "The Emergence of Perovskite Solar Cells" M. A. Green, A. Ho-Baillie and H. J. Snaith *Nature Photonics* 8 (2014) 506–514.

Open-Circuit Voltage Deficit, Radiative Sub-Bandgap States, and Prospects in Quantum Dot Solar Cells

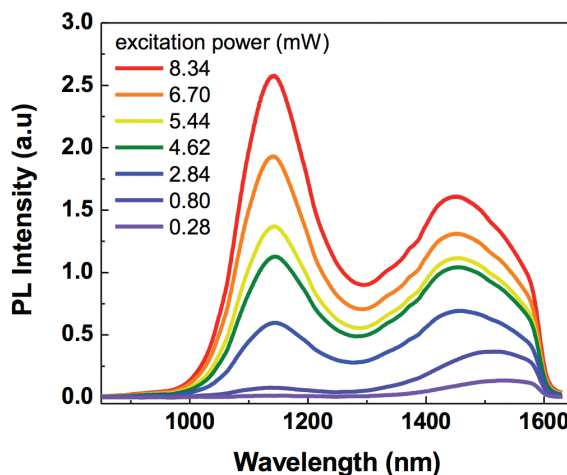
C.-H. M. Chuang, A. Maurano, R. E. Brandt, G. Weon Hwang, J. Jean, T. Buonassisi, V. Bulović, M. G. Bawendi
Sponsorship: Samsung Advanced Institute of Technology

Quantum dot (QD) solar cell based on near-infrared active PbS QDs is an emerging technology that could fulfill the goal of efficient solar energy harvesting at low cost. In addition to the tunable bandgap covering the optimal bandgap ranges for solar cells, PbS QD solar cells can be fabricated with simple solution processes in air at room temperature and exhibit excellent air-stability for over 150 days. However, despite these advantages, the highest efficiency reported so far is still considerably lower than the expected performance for a material with this bandgap range. In this work, we present a comprehensive analysis of our recently developed air-stable PbS QD solar cells with a certified power conversion efficiencies of 8.6%. We

elucidate the carrier recombination mechanisms and the origins of the large open-circuit voltage (V_{OC}) deficit, which is a primary limitation in present QD solar cells. In particular, we show evidence for the presence of radiative sub-bandgap states and the filling of these states in working devices under different operating conditions. We conclude that the performance and V_{OC} of current QD solar cells is mainly limited by these sub-bandgap states rather than the interfaces between QD and other materials. Based on these findings and perspectives on the recent progress of QD solar cells, we discuss future prospects for QD solar and suggest potential routes to improving these devices.



▲ Figure 1: Upper panel: absorption spectra and photoluminescence (PL) spectra of a PbS QD solar cell. Lower panel: J - V characteristics of the certified 8.6%-efficient QD solar cell. The device shows a peak of sub-bandgap emission and a large V_{OC} deficit.



▲ Figure 2: Power-dependent PL spectra of a PbS QD solar cell. The relative intensity of the band-edge emission and sub-bandgap emission changes with excitation power. The progressive blueshift of the sub-bandgap emission is consistent with the sub-bandgap state-filling from deeper states.

FURTHER READING

- C.-H. M. Chuang, P. R. Brown, V. Bulović, and M. G. Bawendi, "Improved performance and stability in quantum dot solar cells through band alignment engineering", *Nature Materials*, vol. 13, p.796, 2014.
- C.-H. M. Chuang, A. Maurano, R. E. Brandt, G. W. Hwang, J. Jean, T. Buonassisi, V. Bulović, and M. G. Bawendi, "Open-Circuit Voltage Deficit, Radiative Sub-Bandgap States, and Prospects in Quantum Dot Solar Cells", *Nano Letters*, vol. 15, p.3286, 2015

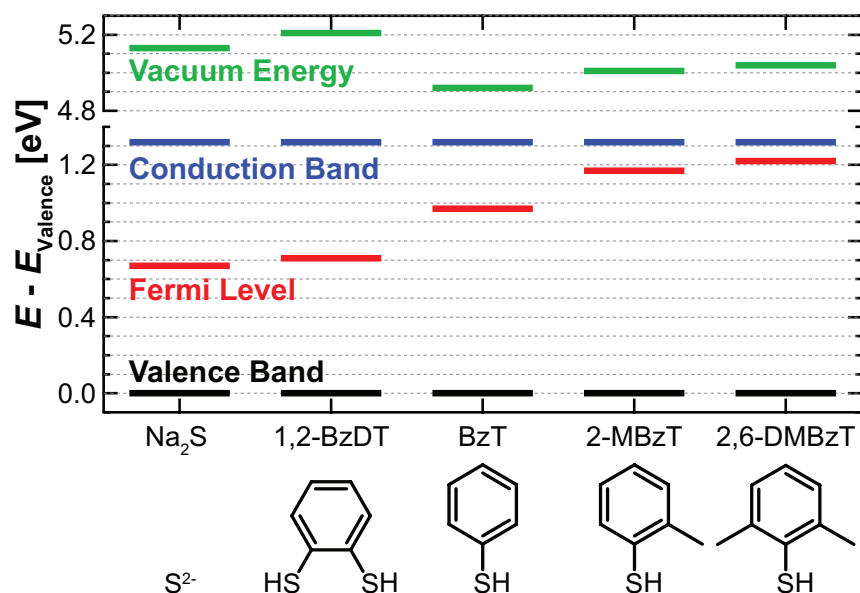
Control of the Fermi Level of Lead Sulfide Quantum Dots through Ligand Steric Interactions

P. R. Brown, V. Bulović

Sponsorship: Samsung, Hertz Foundation, National Science Foundation

The electronic properties of lead sulfide colloidal quantum dots (PbS QDs) can be controlled through modification of the QD surface chemistry via ligand exchange, and recent work from our group has applied ultraviolet photoelectron spectroscopy (UPS) and density functional theory (DFT) to explain the influence of ligand-induced energy-level modification on record-efficiency QD photovoltaics. Control over the QD doping type and doping level is also an important factor in the design of efficient QD photovoltaics. Here, we show that by modifying the steric bulk of sulfur-containing ligands bound to the PbS QD surface, the Fermi level of the QD-ligand complex measured by UPS can be predictably tuned over a range of 0.6 eV within the QD bandgap. As shown in Figure 1, bulkier ligands result

in a Fermi level close to the QD conduction band (signifying n-type behavior), while smaller ligands result in a Fermi level close to the middle of the QD bandgap (signifying intrinsic behavior). This trend is expected given the ionic nature of lead sulfide: an excess of electron-rich lead atoms (realized here using bulky ligands with low relative sulfur content) should lead to n-type doping, while a balanced lead-sulfide ratio (realized here using small sulfide ligands that can effectively passivate the excess lead on the QD surface) should lead to intrinsic behavior. These results identify ligand steric interactions as an important contributor to the stoichiometry and electronic properties of PbS QDs, and as a broadly adjustable parameter in the design of efficient QD optoelectronic devices.



▲ Figure 1: Energy levels of lead sulfide colloidal quantum dots (excitonic absorption peak in solution of $\lambda = 963$ nm) derived from ultraviolet photoelectron spectroscopy and absorption spectroscopy, for five different chemical ligand treatments: sodium sulfide (Na_2S), 1,2-benzenedithiol (1,2-BzDT), benzenethiol (BzT), 2-methylbenzenethiol (2-MBzT), and 2,6-dimethylbenzenethiol (2,6-DMBzT). The chemical structures of the corresponding ligands are shown below the x-axis.

FURTHER READING

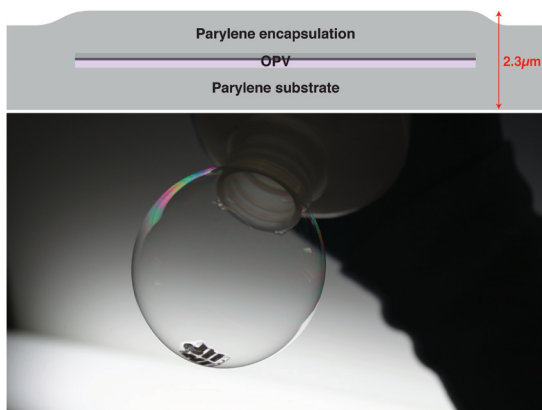
- D. Kim, D.-H. Kim, J.-H. Lee, and J. C. Grossman, "Impact of Stoichiometry on the Electronic Structure of PbS Quantum Dots," *Physical Review Letters*, vol. 110, no.19, pp. 196802-1 – 196802-5, May 2013.
- P. R. Brown, D. Kim, R. R. Lunt, N. Zhao, M. G. Bawendi, J. C. Grossman, and V. Bulović, "Energy Level Modification in Lead Sulfide Quantum Dot Thin Films through Ligand Exchange," *ACS Nano*, vol. 8, no.6, pp. 5863-5872, May 2014.

In Situ Vapor-Deposited Parylene Substrates for Ultra-Thin, Lightweight Organic Solar Cells

J. Jean, A. Wang, V. Bulović
Sponsorship: Eni-MIT Solar Frontiers Center

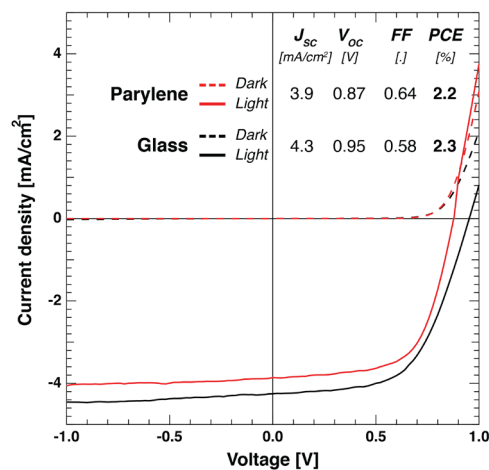
Solar photovoltaics (PV) are among the few low-carbon energy technologies with the scalability to satisfy global electricity demand. Today's leading silicon and thin-film PV modules are low-cost, efficient, and reliable, but also rigid and heavy (~30 kg for a 300 W module). Restricted module form factor limits potential PV applications and contributes to high non-module costs, which dominate total system cost and hinder deployment. Lightweight and flexible solar cells are possible with emerging thin-film technologies, but only if lightweight and flexible substrates are used. In this work, we introduce an alternative approach for producing thin, lightweight, clean, nanoscale-smooth, and flexible PV substrates and encapsulation layers: *in situ* vapor-phase deposition of transparent polymer membranes.

The most common substrate material today is glass: it presents a flat, smooth, robust surface for cell processing and protects sensitive organic and hybrid materials from exposure to oxygen and water vapor. However, a rigid glass sheet dominates cell weight and thickness. For example, typical organic, perovskite, and colloidal quantum dot solar cells are 600–900 nm thick and weigh 3–5 g/m². In contrast, a typical glass substrate or cover is 3 mm thick and weighs ~8 kg/m², dwarfing the mass of the active layers and constraining specific power for a given cell efficiency.



▲ Figure 1: Molecular organic solar cells on 1-µm-thick parylene-C. Top: Device structure with thicknesses shown to scale. Bottom: Picture of parylene-based solar cells supported by a soap bubble, highlighting their low weight and conformability.

Here we demonstrate ultra-thin, lightweight, and flexible solar cells that are uniquely built by growing *in situ* thin polymer films as substrates and fabricating devices on top (Figure 1). For our polymer substrate we use chemical-vapor-deposited poly(chloro-p-xylylene) (parylene-C) films with thicknesses below 1 micron. The solar cells consist of vapor-deposited metal oxides, molecular organic films, and metal electrodes. Encapsulation with parylene-C is similarly performed under vacuum conditions. The entire cell can thus be fabricated without breaking vacuum. In-vacuum processing avoids exposure of substrate surfaces to atmospheric conditions, minimizing contamination and damage risk associated with transportation, handling, and cleaning of ultra-thin substrates. Organic PV cells on parylene exhibit power conversion efficiencies and device yields comparable to cells on glass substrates (Figure 2). These devices are the thinnest (<1 µm) and lightest (3.6 g/m²) solar cells yet demonstrated, with specific powers exceeding 6 W/g, and they illustrate the lower limits of PV substrate thickness and materials use. Solar cells on thin and flexible parylene membranes can be seamlessly adhered onto a variety of solid surfaces, providing for additive solar power on any surface.



▲ Figure 2: Current–voltage characteristics in dark and under 100 mW cm⁻² solar illumination for organic solar cells on glass and on parylene substrates.

FURTHER READING

- J. Jean, A. Wang, and V. Bulović, "In Situ Vapor-Deposited Parylene Substrates for Ultra-thin, Lightweight Organic Solar Cells," submitted.
- J. Jean, P. R. Brown, R. L. Jaffe, T. Buonassisi, and V. Bulović, "Pathways for Solar Photovoltaics," *Energy & Environmental Science*, vol. 8, pp. 1200–1219, Feb. 2015.

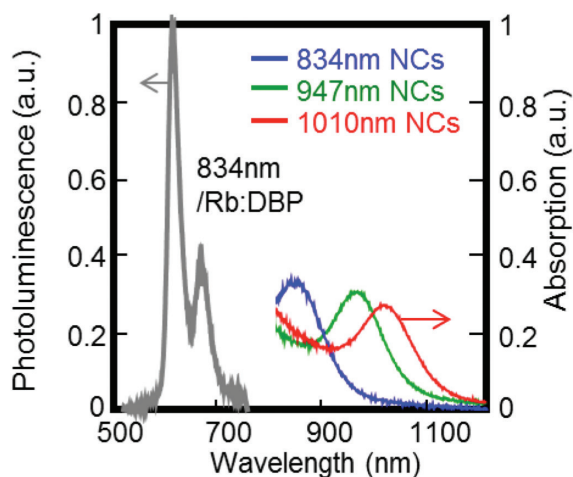
Solid State Triplet-Triplet Annihilation Upconversion

D. N. Congreve, M. Wu, Mark W. B. Wilson, J. Jean, N. Geva, M. Welborn, T. Van Voorhis, V. Bulović, M. G. Bawendi, M. A. Baldo
Sponsorship: Department of Energy, Basic Energy Sciences, DE-SC0001088

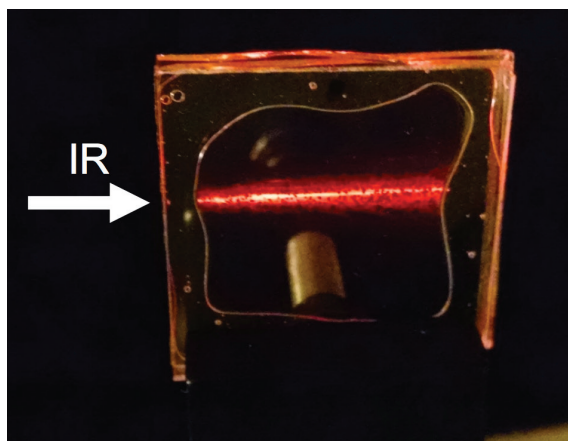
Despite decades of research, silicon photovoltaics have peaked at power efficiencies of approximately 25%. This loss is largely due to two unavoidable processes: the thermalization of high energy photons and the transmission of low energy photons. Here, we propose a cost effective, straightforward method for increasing photovoltaic power efficiencies past the Shockley Queisser limit. Upconversion is the process of turning two low energy photons into one high energy photon. When applied to silicon, upconversion can add substantial power gains without increasing the complexity of the solar cell. The upconverting layer can be applied to the back of the photovoltaic, capturing un-absorbed photons and returning them to the silicon cell as absorbable ones.

Here, we demonstrate upconversion using colloidal nanocrystals as the sensitizer and the organic material

rubrene as the annihilator. The addition of 0.5% of a dopant dye allows for a 20-fold increase in the photoluminescence. The energetics of this process are illustrated in Figure 1. Light is absorbed by the nanocrystals at up to 1000 nm. The nanocrystals generate triplet states which transfer to the rubrene, where they undergo triplet-triplet annihilation to generate a singlet state and fluoresce; Figure 1, grey. The utilization of nanocrystals allows for further reach into the infrared as compared with current state of the art devices. Further, they minimize energy loss in the intersystem crossing process, allowing for a greater energetic difference between absorbed and emitted light. The successful application of upconversion to a silicon solar cell could increase efficiencies from 25% to over 30%.



▲ Figure 1: Energetics of upconversion. The light is absorbed by the nanocrystals (red, green, blue) and converted to triplet states, which transfer to the rubrene. They undergo triplet-triplet annihilation and then fluoresce from the emitter molecule, grey curve.



▲ Figure 2: Visible demonstration of upconversion. The sample is excited by an 808 nm laser beam from the left. Red fluorescence from the emitter is observed.

FURTHER READING

- T. Singh-Rachford and F. Castellano, "Photon Upconversion based on sensitized triplet-triplet annihilation", *Coordination Chemistry Review*, vol. 254, pp. 2560-73, 2010.

Thin Film Evaporation from Nanopores and its Applications to Solar Thermal Devices

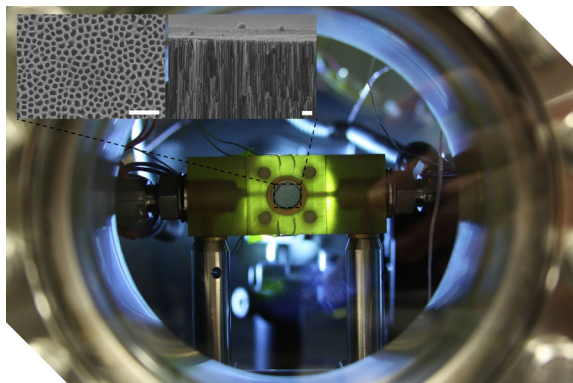
K. L. Wilke, B. Barabadi, E. N. Wang
Sponsorship: Masdar Institute/MIT Cooperative Program

The continuous growth of demands for energy and clean water, dwindling resources, and the environmental impact of the current techniques that dominate the world's energy market make the need for alternative, renewable sources as prominent as ever. Given solar energy's theoretical energy potential is 89,300 TW only a very small fraction of the available solar energy would be needed to provide our current needs.

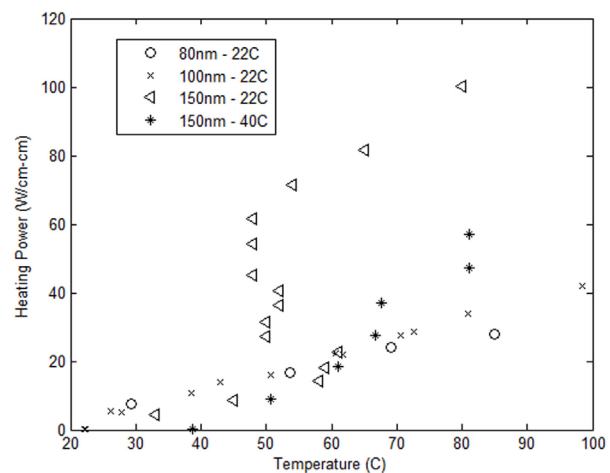
In this work, we consider solar thermal energy where the key process is the conversion of light to heat to vapor. The produced vapor could be utilized for the production of electricity or distilled water, etc. Recently, it was shown that as much 80% of absorbed sunlight could be converted to water vapor by using absorptive nanoparticles dispersed in water. It was suggested that localized heating of the nanoparticles allowed the high efficiency conversion and prevented heat from being lost to the surroundings. We have expanded this idea of localized energy absorption and conversion to a concept that may have more practical relevance than a nanofluid. The surface of a nanoporous membrane is coated with a thin layer to absorb the sunlight. Liquid is wicked in via capillarity from the bottom of the membrane and forms a meniscus near the absorbing layer. As light is absorbed, heat is generated in the thin absorbing film near the liquid-vapor interface of the meniscus. Because

the meniscus is in a nanopore, the conduction resistance from the pore wall through the liquid to the evaporating interface is small, and the efficient heat transfer of thin film evaporation can be utilized. As the input heat flux varies, the shape of the meniscus changes to increase or decrease the capillary pressure, providing passive pumping of the liquid. Furthermore, the membrane can be thermally insulating to prevent thermal losses to the liquid below.

To study device characteristics and gain a fundamental understanding of evaporation through nanoporous structures, we designed and fabricated a series of nanoporous membranes. Parameters such as pore diameter, porosity, and location of the meniscus within the pore can be varied. An experimental setup to test the evaporation from the membranes has been built (see Figure 1 for image of test fixture and SEM images of membranes), and suitability to different solar thermal devices is considered. We believe this study will provide understanding of solar-driven evaporation with highly localized heating, as well as a fundamental understanding of how parameters such as pore size and location of the meniscus affect evaporation from nanopores, some initial results of which are shown in Figure 2. During tests the input power, evaporation rate, surface temperature, and other parameters are monitored.



▲ Figure 1: Test fixture seen from a viewport in the experimental vacuum chamber. Insets show SEM images of the anodic aluminum oxide membranes used for evaporation tests. Scale bars: 1µm



▲ Figure 2: Surface temperature vs. heating power for samples of different pore diameter and different chamber ambient temperatures.

FURTHER READING

- J. Tsao, N. Lewis, and G. Crabtree. (2006, Apr.) Solar FAQs. [Online]. Available: <http://www.sandia.gov/~jytsao/Solar%20FAQs.pdf>
- O. Neumann, A. Urban, J. Day, S. Lal, P. Nordlander, N. Halas "Solar vapor generation enabled by nanoparticles," *ACS Nano*, vol. 7, no. 1, pp. 42-49, Nov. 2012.

MEMS Energy Harvesting from Low-Frequency and Low-G Vibrations

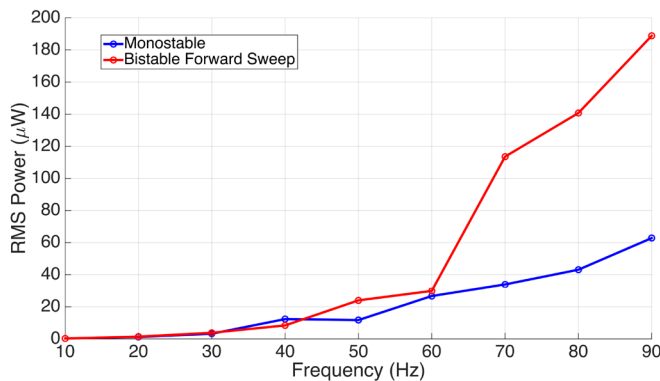
R. Xu, S.G. Kim

Sponsorship: MIT-SUTD International Design Center

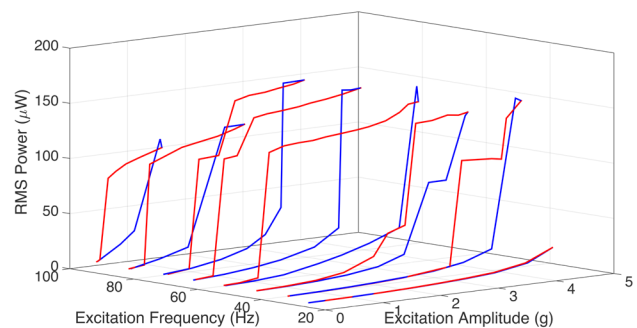
MEMS-scale vibration energy harvesting has been investigated for more than a decade to enable autonomous systems such as batteryless wireless sensor networks. Toward this goal, a fully assembled energy harvester at a size of a quarter dollar coin should be able to generate robustly about 100 mW continuous power from ambient vibration (mostly less than 100Hz and 0.5g acceleration) with reasonably wide bandwidth (>20%). We are inching close toward this goal in terms of power density and bandwidth, but not in terms of low frequency operations.

Most of the reported vibration energy harvesters use a linear cantilever resonator structure to amplify small ambient vibration. While such structures are easy to model, design and build, they typically have a narrow bandwidth. In contrast, nonlinear resonators have different dynamic response and greatly increase the bandwidth by hardening or softening the resonance characteristic of the beam structure. In addition, it has been found that non-linear resonating stretching beams can extract more electrical energy than linear resonating bending beams can. Our previous research with non-linear resonating stretching energy harvesters achieved 2.0 mW/mm³ power density with >20% power bandwidth. But it was operated with input vibrations of >1 KHz and 4.0 g acceleration, which practically limits the use of this technology, harvesting energy from real environmentally available vibrations. Many believed this is an inherent limitation imposed on the MEMS scale structures.

We approached this problem with a bi-stable nonlinear resonating buckled beam. Compared to mono-stable nonlinear resonance, we found bi-stable resonance could bring more dynamics phenomena to help reduce the operating frequency as well as the g-requirement. Electromechanical lumped model has been built for simulating the dynamics of buckled clamped-clamped beam structure. The two oscillation modes, intra-well and inter-well with respect to the double energy well potential of the bi-stable system, have been predicted. We also found the characteristic spring softening and spring stiffening responses, which were associated with the small-amplitude intra-well and large-amplitude inter-well oscillations respectively. In order to validate the simulated models, a meso-scale prototype has been built and tested on an electromagnetic shaker with controlled and monitored input vibration frequency and amplitude. The testing results verify the theoretical predictions, showing a shifted response of bi-stable configuration, which generates more power than the mono-stable configuration at lower frequencies (Figure 1). Hysteresis also exists when varying the vibration amplitude at fixed frequency, so that at low g input, the bi-stable energy harvesters still generate a significant amount of power (Figure 2). The buckled bi-stable beam structure is believed to solve the last challenge of the MEMS energy harvester at low frequency and low-g input vibrations. The MEMS device will be fabricated soon.



▲ Figure 1: Power frequency responses of mono-stable and bi-stable configurations of the same setup at 3g excitation.



▲ Figure 2: The input acceleration amplitude was swept forward (blue) and backward (red) at fixed frequencies from 30Hz to 100Hz for the same bi-stable system.

FURTHER READING

- R. Xu and S.G. Kim, "MEMS Energy Harvesting from Low-Frequency and Low-Gg Vibrations," in *2015 MRS Spring Meeting*, 2015.
- A. Hajati and S.G. Kim, "Ultra-wide bandwidth piezoelectric energy harvesting," *Appl. Phys. Lett.*, vol. 99, no. 8, p. 083105, 2011.

Fabrication of Ruthenium Oxide-Coated Si Nanowire-Based Supercapacitors

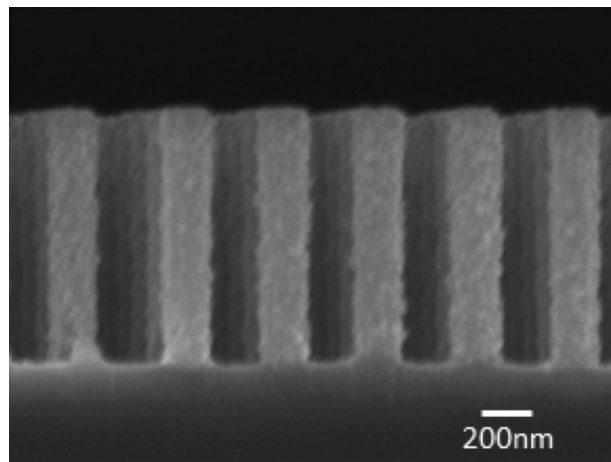
W. Zheng, J. Xie, D. Wang, C. V. Thompson

Sponsorship: Singapore-MIT Alliance for Research and Technology

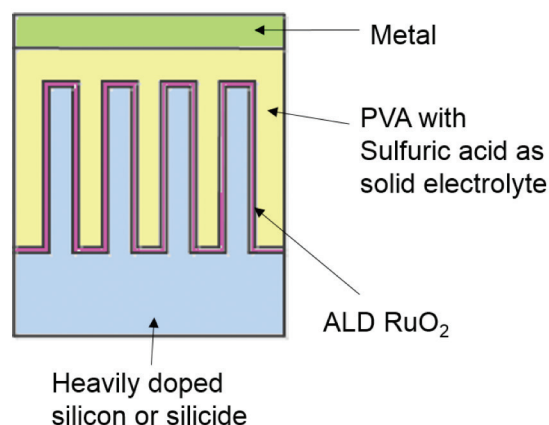
Supercapacitors are electrochemical devices that have high power density and long cycle life. Pseudo-capacitors are a type of supercapacitor that involves reversible surface reduction/oxidation reactions. Among all the pseudo-capacitive materials, ruthenium oxide is the most promising due to its high specific capacitance, excellent cyclability, and high conductivity. While researchers have been developing supercapacitors based on ruthenium oxide or its composite with other materials such as CNT, there has been little study on ruthenium oxide-Si composite. In earlier work, we demonstrated the feasibility of using metal-assisted chemical etching (MACE) to fabricate Si nanowires for on-chip MOS capacitors. Here we continue using an ordered vertical array of Si nanowires from MACE to fabricate on-chip supercapacitors.

Atomic layer deposition (ALD) is used to deposit ruthenium oxide on silicon nanowires due to its conformal coating on high aspect ratio structures. Moreover, it also provides a precise control of the

ruthenium oxide film thickness. As pseudo-capacitive reactions occur at the surface of ruthenium oxide, the high aspect ratio Si nanowire structure coated with ruthenium oxide has a highly accessible ruthenium oxide surface area and thus leads to a high energy storage capacitance. We have developed an ALD process for conformal coating of ruthenium oxide on silicon nanowires generated by MACE. The composite structure shows a coating of well-distributed particles (Figure 1). High-resolution transmission electron microscopy (HRTEM) characterization confirmed that these particles match the lattice of ruthenium oxide. We are currently investigating the electrochemical performance of this composite material using a three-electrode set up. Meanwhile, we are optimizing the ALD process according to the measured electrochemical performance. Our ultimate goal is to fabricate a solid state micro on-chip supercapacitor based on the optimized electrode material (Figure 2).



▲ Figure 1: SEM image of an array of Si pillars after ALD of ruthenium oxide.



▲ Figure 2: Schematic of the solid state micro on-chip supercapacitor.

FURTHER READING

- S. W. Chang, J. Oh, S. T. Boles, and C. V. Thompson, "Fabrication of Silicon Nanopillar-Based Nanocapacitor Arrays," *Applied Physics Letters*, vol. 96, pp. 153108, 2010.
- S. W. Chang, V. P. Chuang, S. T. Boles, C. A. Ross, and C. V. Thompson, "Densely-Packed Arrays of Ultrahigh-Aspect-Ratio Silicon Nanowire Fabricated Using Block Copolymer Lithography and Metal-Assisted Etching," *Advanced Functional Materials*, vol. 19, pp. 2495-2500, 2009.

Materials and Structures for Lithium-Air Batteries

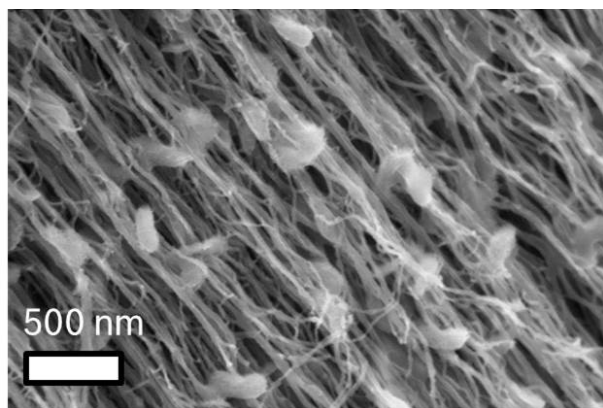
T. Batcho, D. Li, D. Kwabi, R. Omampuliyur, Y. Shao-Horn, C. V. Thompson
Sponsorship: Bosch, Skoltech Center for Electrochemical Energy Storage

Lithium-air batteries hold promise for the next generation of electric vehicles and other applications. By reacting oxygen directly with lithium ions to form Li_2O_2 on discharge, they can achieve energy densities 3-5 times higher than current lithium-ion batteries. However, a number of challenges exist for implementing lithium-air batteries, including poor rate capability, poor cyclability, high overpotentials upon charging and electrode and electrolyte instability. We seek to address these issues by developing new electrode materials and architectures and performing studies of Li_2O_2 formation under various discharge conditions.

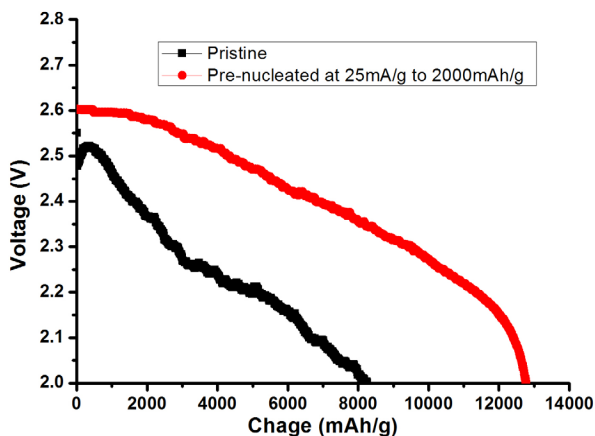
Aligned arrays of carbon nanotubes (CNTs) provide ideal conductive scaffolding materials for Li_2O_2 while occupying a small volume fraction and having low mass. CNTs of 5-10 nm in diameter are grown in aligned forests on a catalyst-deposited silicon wafer and delaminated. These free-standing carpets can be placed directly into our cell. We observed nearly ideal gravimetric capacities and high volumetric capacities. However, carbon has been found to decompose in lithium-air cells and promote electrolyte decomposition. These side reactions lead to

poor cycling performance and high overpotentials on charge. In order to avoid these effects, we have worked on depositing coating materials such as TiN onto CNTs to chemically passivate the carbon surface (see Figure 1). We are able to completely coat the CNTs and are currently working on optimizing conductivity and testing electrochemical performance.

The rate capability of Li-air battery with CNTs cathode is still not satisfying. The current understanding of the mechanism is that Li_2O_2 forms different morphologies at different rates. As an insulator material, Li_2O_2 forms a uniform coating on CNTs at a high rate and passivates the electron transport, leading to a limited capacity. At a low rate, Li_2O_2 forms toroidal particles and results in a much larger capacity. To further understand the discharge product nucleation and growth mechanism and to exploit the full potential of Li-air battery application, we pre-nucleate particles at a low rate and then discharge them at a high rate to try to optimize capacity and void-filling and learn about nucleation and growth mechanisms (see Figure 2).



▲ Figure 1: SEM micrograph of toroidal Li_2O_2 formation on CNTs deposited with a coating of TiN.



▲ Figure 2: Discharge diagram at 500mA/g of pristine CNTs and CNTs pre-nucleated at 25mA/g to 2000mAh/g.

FURTHER READING

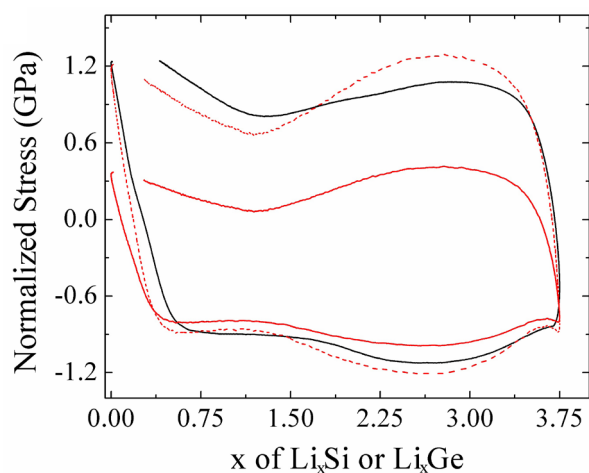
- Y. C. Lu, B. M. Gallant, D. G. Kwabi, J. R. Harding, R. R. Mitchell, M. S. Whittingham, and Y. Shao-Horn, "Lithium-oxygen batteries: bridging mechanistic understanding and battery performance," *Energy and Environmental Science*, vol. 6, p. 750-768, Jan. 2013.
- R. R. Mitchell, B. M. Gallant, Y. Shao-Horn, and C. V. Thompson, "Mechanisms of Morphological Evolution of Li_2O_2 Particles during Electrochemical Growth," *Journal of Physical Chemistry Letters*, vol. 4, no. 7, p. 1060, Mar. 2013.

Mechanical Stresses in Germanium Thin Film Microbattery Electrodes during Cycling

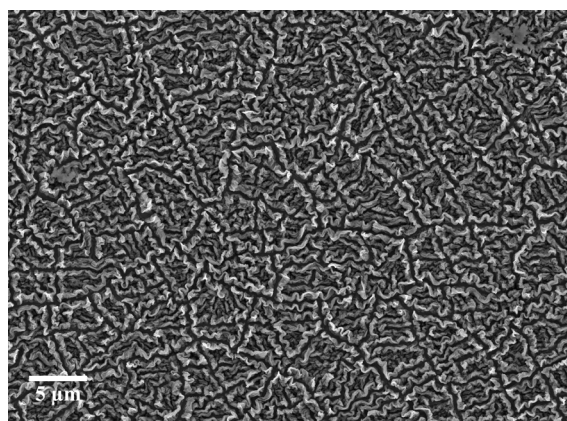
A. Al-Obeidi, D. Kramer, R. Moenig, C. V. Thompson
Sponsorship: Singapore-MIT Alliance for Research and Technology

A critical component for autonomous microsystems is a reliable energy storage system that can be integrated with on-board energy harvesting and power management systems. One possible energy storage system to meet this demand is lithium-ion thin film microbatteries, which offer high energy storage capacities. For the anode, silicon and germanium offer capacities as high as 3579 A h kg^{-1} and 1384 A h kg^{-1} compared to graphite's theoretical capacity of only 372 A h kg^{-1} . However, use of these materials has been limited by the significant volumetric and structural changes that occur during cycling. In order to explore the relationship between electrochemistry and the mechanical stresses that arise, *in situ* stress measurements on thin film electrodes were conducted.

It was found that the stresses developed in 90 nm thick germanium films were lower than in silicon by roughly one-third (Figure 1) and showed better capacity retention at higher rates. Cycling thicker 170 nm films initially showed similar stress behavior to that of the thinner 90 nm films but showed a significant drop in stress magnitude with cycling. Imaging these cycled films showed that the initially continuous thin film had evolved toward a complex, three-dimensional island structure, which had lower stress (Figure 2). The reduced plastic flow stresses observed in lithium-germanium and the weak dependence on charge-discharge rates correlate with the improved cyclability and reduced rate sensitivity found in germanium electrodes as compared to silicon.



▲ Figure 1: Evolution of stress as a function of anode capacity for silicon and germanium.



▲ Figure 2: Low magnification SEM image of an extensively cycled 170 nm germanium film.

FURTHER READING

- Z. Choi, D. Kramer, and R. Mönig, "Correlation of stress and structural evolution in $\text{Li}_4\text{Ti}_5\text{O}_{12}$ -based electrodes for lithium ion batteries," *Journal of Power Sources*, vol. 240, pp. 245-251, Oct. 2013.

Oxygen Exchange Kinetics in Pr_2CuO_4 Thin Film Cathodes: The Role of Doping and Orientation

K. Mukherjee, H. L. Tuller (in collaboration with Y. Hayamizu, S. Istomin)
Sponsor: Skolkovo Foundation

Layered oxide compounds with mixed ionic electronic conductivity are promising candidate materials for cathodes in intermediate-temperature solid oxide fuel cells. There have been reports of anisotropic oxygen ion conductivity in materials with the K_2NiF_4 (T) and Nd_2CuO_4 (T') crystal structures, with facile transport along the rock-salt layers. These material systems also exhibit anisotropic thermal and chemical expansion properties, potentially important for long-term device stability. However, in practice, it is difficult to control the crystal structure, doping and grain orientation independent of each other to understand their effect on cathode performance. Additionally, the lanthanide cuprates exhibit a third phase (T*), a hybrid of the T and T' phases with important implications for the ionic and electronic conductivity.

In this work, we synthesized thin films of Pr_2CuO_4 with varying amounts of Sr and Ce doping using pulsed-laser deposition on single crystal YSZ substrates. Alloys with the same crystal structure and doping but with different film orientations were also successfully synthesized through the use of seed layers on YSZ. Using electrochemical impedance spectroscopy to measure the area-specific resistance, we find a significant improvement in the oxygen surface-exchange rate as a result of both donor and acceptor doping. However, the activation energies are very different, indicative of different rate-determining steps in each case.

FURTHER READING

- M. Burriel, G. Garcia, J. Santiso, J. A. Kilner, R. J. Chater, and S. J. Skinner, "Anisotropic oxygen diffusion properties in epitaxial thin films of $\text{La}_2\text{NiO}_{4+\delta}$," *Journal of Materials Chemistry*, vol. 18, no. 4, pp. 416-422, Jan. 2008.
- G. N. Mazo, Yu. A. Mamaev, M. Z. Galin, M. S. Kaluzhskikh, A. K. Ivanov-Schitz, "Structural and transport properties of the layered cuprate Pr_2CuO_4 ," *Inorganic Materials*, vol. 47, no. 11, pp. 1218-1226, Oct. 2011.

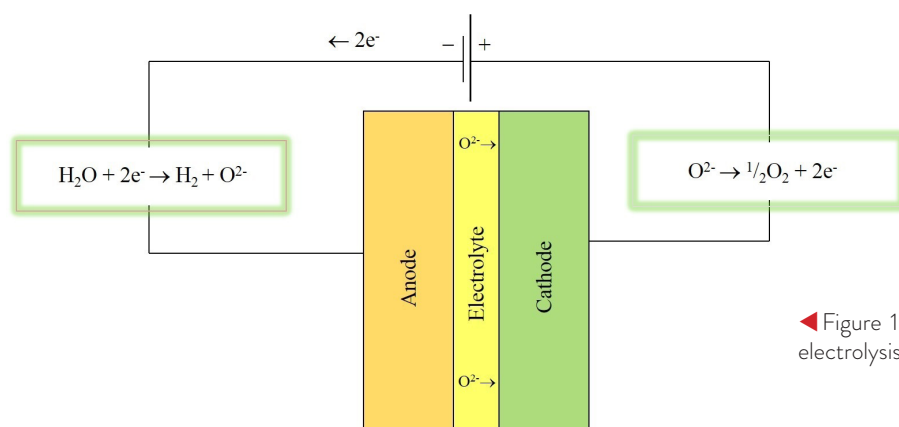
Development of Reversible Solid Oxide Cells: A Search for New Electrode Materials

C. S. Kim, S. R. Bishop, H. L. Tuller
Sponsorship: Skolkovo Foundation

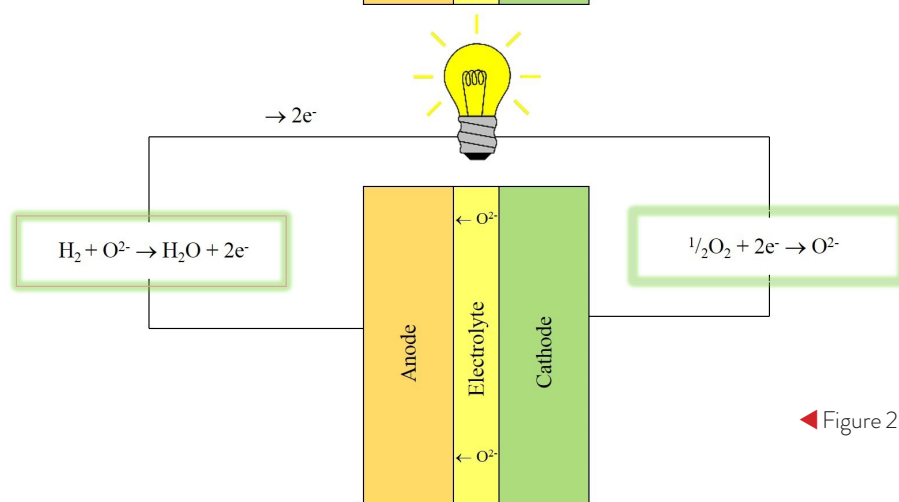
Recent advances in photovoltaic cells have enabled efficient conversion of solar energy to electricity at low cost. However, solar radiation is intermittent, and an efficient means for storage of excess electricity generated during daytime is needed. Electrolysis cells can convert excess electrical energy into chemical fuels via the electrolysis of water (H_2O) or carbon dioxide (CO_2) to hydrogen (H_2) or carbon monoxide (CO), respectively, with the excess stored energy converted back to electricity efficiently by solid oxide fuel cells (SOFCs). A reversible SOFC can operate as an electrolysis cell (Figure 1) during the day and as a fuel cell (Figure 2) at night. While symmetric solid oxide cells with redox stable electrodes have been investigated, their performance is substantially lower than the state-of-the-art SOFCs. In

this project, we are investigating new redox stable electrode materials with high mixed (electrical and ionic) conductivity under both highly oxidizing and reducing conditions.

The defect structure and transport properties of new candidate electrode materials are investigated by thermogravimetry, electrical conductivity, and dilatometry as functions of temperature and oxygen partial pressure. Surface kinetics are examined by means of ac impedance spectroscopy of half-cells and symmetric cells fabricated by depositing electrode materials onto electrolytes by pulsed laser deposition. Electrode performance is being correlated with defect and transport models developed on the basis of the collected thermodynamic and kinetic experimental data.



◀ Figure 1: A reaction diagram of a solid oxide electrolysis cell.



◀ Figure 2: A reaction diagram of an SOFC.

FURTHER READING

- A. Hauch, S. H. Jensen, S. Ramousse, and M. Mogensen, "Performance and Durability of Solid Oxide Electrolysis Cells," *Journal of the Electrochemical Society*, vol. 153, no. 9, pp. A1741-A1747, July 2006.

Investigation of Fuel Cell Cathode Performance in Solid Oxide Fuel Cells: Application of Model Thin Film Structures

J. J. Kim, D. Chen, N. Perry, S. R. Bishop, H. L. Tuller
Sponsorship: Department of Energy

An improved fundamental understanding of oxygen nonstoichiometry (δ) and surface exchange kinetics in solid oxide fuel cell (SOFC) cathodes is considered to be critical for achieving enhanced device performance and longevity, especially at reduced operating temperatures. Although numerous research activities have been focused on elucidating the oxygen reduction reaction (ORR) mechanisms at the cathode, their conclusions remain unsatisfactory and controversial. The ORR at mixed conducting oxide thin film cathodes consists of oxygen adsorption, dissociation, charge-transfer, incorporation, and migration of charge carriers. The kinetic parameters associated with the overall ORR, such as the diffusion coefficient (D) and surface exchange coefficient (k), are strongly influenced by δ in the oxides. On the other hand, oxygen defect generation is often associated with valency changes in the transition metal or rare earth ions within the oxides and with corresponding changes in lattice constant (chemical expansion). This expansion may lead to stresses sufficient to support crack initiation and/or delamination, impacting the device's long-term stability. Because many advanced oxide materials used in

SOFC experience significant changes in δ during operation at elevated temperatures and under reducing/oxidizing conditions, the ability to diagnose a material's behavior *in situ* is therefore important.

Our group recently demonstrated that δ in $\text{Pr}_{0.1}\text{Ce}_{0.9}\text{O}_{2-\delta}$ (10 PCO) thin films could be reliably derived by utilizing chemical capacitance extracted from electrochemical impedance spectroscopy (EIS) measurements. Furthermore, we have introduced a non-contact optical means for *in situ* recording of transient redox kinetics, as well as the equilibrium Pr oxidation state and, in turn, δ in 10 PCO thin films, by monitoring the change in absorption spectra upon change in $p\text{O}_2$ or temperature. In this study, we are investigating cathode kinetics and nonstoichiometry of two model oxide thin films, $\text{Sr}(\text{Ti},\text{Fe})\text{O}_{3-\delta}$ (STF) with Ba or La doping and $(\text{Pr},\text{Ce})\text{O}_{2-\delta}$ (PCO), by simultaneously utilizing *in situ* and *in operando* optical absorption spectroscopy and EIS as a function of temperature, $p\text{O}_2$, and electrical potential. We are also investigating changes in surface chemistry and their impact on electrode impedance by atomic force microscopy (AFM), x-ray photoelectron spectroscopy (XPS), and low-energy ion-scattering spectroscopy (LEIS).

FURTHER READING

- D. Chen, S. R. Bishop, and H. L. Tuller, "Non-stoichiometry in oxide thin films: a chemical capacitance study of the praseodymium-cerium oxide system," *Adv. Funct. Mater.*, vol. 23, pp. 2168-2174, May 2013.
- J. J. Kim, S. R. Bishop, N. J. Thompson, D. Chen, and H. L. Tuller, "Investigation of nonstoichiometry in oxide thin films by simultaneous *in situ* optical absorption and chemical capacitance measurements: Pr-doped ceria, a case study," *Chem. Mater.*, vol. 26, pp. 1374-1379, Jan. 2014.
- J. J. Kim, S. R. Bishop, N. J. Thompson, and H. L. Tuller, "Investigation of redox kinetics by simultaneous *in situ* optical absorption relaxation and electrode impedance measurements: Pr doped ceria thin films," *ECS Transactions*, vol. 57, no. 1, pp. 1979-1984, 2013.

Fundamental Studies of Oxygen Exchange and Associated Expansion in Solid Oxide Fuel Cell Cathodes

N. H. Perry, J. J. Kim, D. Marrocchelli, S. R. Bishop, H. L. Tuller (in collaboration with B. Yildiz, D. Pergolesi)
Sponsorship: Department of Energy

In order to lower the cost of solid oxide fuel cells (SOFCs), both the low-temperature efficiency and long-term durability need to be improved. Two key areas involving fundamental studies of how fuel cell materials “breathe” oxygen under operating conditions that we are examining are 1) the origin of sluggish oxygen incorporation at the cathode, which often dominates SOFC efficiency losses at low temperatures, and 2) the origin of chemical expansion during oxygen loss from the oxide, which can result in catastrophic mechanical failure of the cell in addition to electro-chemo-mechanical coupling effects. Our recent review article (*Annu. Rev. Mater. Res.*, 44, 2014) highlights the widespread presence of chemical expansion and its consequences across a number of energy conversion and storage devices.

In this work we experimentally and theoretically investigate cathode systems with model geometries (controlled active surface area and diffusion lengths of thin films) and model chemistries (tailored electronic structure, crystal structure, and defect chemistry) to isolate underlying factors controlling the oxygen

exchange and expansion behavior. Previous work on fluorite-structured electrodes is being extended to the perovskite families $(\text{Sr,Ba,Ca,La})(\text{Ti,Fe,Co})\text{O}_{3-\delta}$ and $(\text{La,Sr})(\text{Ga,Ni})\text{O}_{3-\delta}$, using advanced *in situ* X-ray diffraction, optical absorption, thermogravimetric analysis, dilatometry, and electrochemical impedance spectroscopy techniques, defect thermodynamic modeling, and density functional theory calculations. Using this approach we have experimentally confirmed our previous theoretical calculations demonstrating the important role of charge localization in controlling chemical expansion behavior. We have also identified other key factors, such as temperature, crystal symmetry, and oxygen vacancy radii, which impact chemical expansion in perovskites. In related studies, we have demonstrated how chemical substitution affects defect chemistry, electronic structure, and corresponding oxygen exchange rate at the cathode surface. Such information is key to the design of both efficient and durable fuel cell electrodes.

FURTHER READING

- N. H. Perry, S. R. Bishop, and H. L. Tuller, “Tailoring Chemical Expansion by Controlling Charge Localization: *In Situ* X-ray Diffraction and Dilatometric Study of $(\text{La,Sr})(\text{Ga,Ni})\text{O}_{3-\delta}$ Perovskite,” *Journal of Materials Chemistry A*, vol. 2, p. 18906-18916, 2014.
- N. H. Perry, J. J. Kim, S. R. Bishop, and H. L. Tuller, “Strongly Coupled Thermal and Chemical Expansion in the Perovskite Oxide System $\text{Sr}(\text{Ti,Fe})\text{O}_{3-\alpha}$,” *Journal of Materials Chemistry A*, vol. 3, p. 3602-3611, 2015.
- N. H. Perry, D. Pergolesi, S. R. Bishop, and H. L. Tuller, “Defect chemistry and surface oxygen exchange kinetics of La-doped $\text{Sr}(\text{Ti,Fe})\text{O}_{3-\alpha}$ in oxygen-rich atmospheres,” *Solid State Ionics*, vol. 273, p. 18-24, 2015.

